

Accepted Manuscript

Decorin Regulates Cartilage Pericellular Matrix Micromechanobiology

Daphney R. Chery, Biao Han, Ying Zhou, Chao Wang, Sheila M. Adams, Prashant Chandrasekaran, Bryan Kwok, Su-Jin Heo, Motomi Enomoto-Iwamoto, X. Lucas Lu, Dehan Kong, Renato V. Iozzo, David E. Birk, Robert L. Mauck, Lin Han

PII: S0945-053X(20)30104-9
DOI: [doi:10.1016/j.matbio.2020.11.002](https://doi.org/10.1016/j.matbio.2020.11.002)
Reference: MATBIO 1659

Published in: *Matrix Biology*

Received date: 2 September 2020
Revised date: 17 November 2020
Accepted date: 17 November 2020

Cite this article as: Chery DR, Han B, Zhou Y, Wang C, Adams SM, Chandrasekaran P, Kwok B, Heo S-J, Enomoto-Iwamoto M, Lu XL, Kong D, Iozzo RV, Birk DE, Mauck RL, Han L, Decorin Regulates Cartilage Pericellular Matrix Micromechanobiology, *Matrix Biology*, [doi:10.1016/j.matbio.2020.11.002](https://doi.org/10.1016/j.matbio.2020.11.002)

This is a PDF file of an unedited manuscript that has been accepted for publication. As a service to our customers we are providing this early version of the manuscript. The manuscript will undergo copyediting, typesetting, and review of the resulting proof before it is published in its final form. Please note that during the production process errors may be discovered which could affect the content, and all legal disclaimers that apply to the journal pertain.

Highlights

- Decorin regulates the aggrecan network integrity and micromechanics of cartilage pericellular matrix.
- The highly negative charged osmotic microenvironment of pericellular matrix is required for normal chondrocyte mechanotransduction *in situ*.
- Decorin affects the intracellular calcium signaling of chondrocytes by mediating the aggrecan-endowed osmotic microenvironment of pericellular matrix.
- The impact of decorin loss on the disruption of chondrocyte mechanobiology is increasingly aggravated during maturation.

Journal Pre-proof

Decorin Regulates Cartilage Pericellular Matrix

Micromechanobiology

*Daphney R. Chery^a, Biao Han^a, Ying Zhou^b, Chao Wang^a, Sheila M. Adams^c,
 Prashant Chandrasekaran^a, Bryan Kwok^a, Su-Jin Heo^{d,e}, Motomi Enomoto-Iwamoto^f, X. Lucas Lu^g,
 Dehan Kong^b, Renato V. Iozzo^h, David E. Birk^c, Robert L. Mauck^{d,e}, and Lin Han^{a,*}*

^aSchool of Biomedical Engineering, Science and Health Systems, Drexel University,
 Philadelphia, PA 19104, United States

^bDepartment of Statistical Sciences, University of Toronto, Toronto, ON M5S 3G3, Canada

^cDepartment of Molecular Pharmacology and Physiology, Morsani School of Medicine,
 University of South Florida, Tampa, FL 33612, United States

^dMcKay Orthopaedic Research Laboratory, Department of Orthopaedic Surgery, Perelman School of
 Medicine, University of Pennsylvania, Philadelphia, PA 19104, United States

^eTranslational Musculoskeletal Research Center, Corporal Michael J. Crescenz Veterans Administration
 Medical Center, Philadelphia, PA 19104, United States

^fDepartment of Orthopaedics, School of Medicine, University of Maryland,
 Baltimore, MD 21201, United States

^gDepartment of Mechanical Engineering, University of Delaware,
 Newark, DE 19716, United States

^hDepartment of Pathology, Anatomy, and Cell Biology, Sidney Kimmel Medical College,
 Thomas Jefferson University, Philadelphia, PA 19107, United States

Running Title: Decorin in Cartilage Pericellular Matrix Micromechanobiology

*Correspondence to Lin Han: lh535@drexel.edu.

For submission to *Matrix Biology* as a *Regular Research Paper*.

Declarations of Interest: None.

Abstract

In cartilage tissue engineering, one key challenge is for regenerative tissue to recapitulate the biomechanical functions of native cartilage while maintaining normal mechanosensitive activities of chondrocytes. Thus, it is imperative to discern the micromechanobiological functions of the pericellular matrix, the ~ 2-4 μm -thick tissue domain in immediate contact with chondrocytes. In this study, we discovered that decorin, a small leucine-rich proteoglycan, is a key determinant of cartilage pericellular matrix micromechanics and chondrocyte mechanotransduction *in vivo*. The pericellular matrix of decorin-null murine cartilage developed reduced content of aggrecan, the major chondroitin sulfate proteoglycan of cartilage and a mild increase in collagen II fibril diameter *vis-à-vis* wild-type controls. As a result, decorin-null pericellular matrix showed a significant reduction in micromodulus, which became progressively more pronounced with maturation. In alignment with the defects of pericellular matrix, decorin-null chondrocytes exhibited decreased intracellular calcium activities, $[\text{Ca}^{2+}]_i$, in both physiologic and osmotically evoked fluidic environments *in situ*, illustrating impaired chondrocyte mechanotransduction. Next, we compared $[\text{Ca}^{2+}]_i$ activities of wild-type and decorin-null chondrocytes following enzymatic removal of chondroitin sulfate glycosaminoglycans. The results showed that decorin-mediated chondrocyte mechanotransduction primarily through regulating the integrity of the aggrecan network, and thus, aggrecan-endowed negative charge microenvironment in the pericellular matrix. Collectively, our results provide robust genetic and biomechanical evidence that decorin is an essential constituent of the native cartilage matrix, and suggest that modulating decorin activities could improve cartilage regeneration.

Keywords:

Pericellular matrix, decorin, chondrocyte, nanomechanics, mechanotransduction.

INTRODUCTION

A key paradox in cartilage regeneration is that while a soft mechanical environment is required for maintaining chondrocyte phenotype [1], a much higher modulus is needed for engineered products to recapitulate the function of native tissue [2]. When cultured *in vitro*, chondrocytes are encapsulated in soft hydrogels with modulus \sim 10 kPa or less to maintain cell viability and prevent de-differentiation [1]. In this environment, while chondrocytes can synthesize major cartilage extracellular matrix (ECM) constituents, namely type II collagen and aggrecan, these molecules do not assemble into the hierarchical structure of the native ECM, thereby failing to fully restore the biomechanical properties of native tissue [3]. *In vivo*, chondrocytes reside within the pericellular matrix (PCM), a structurally distinctive, \sim 2-4 μ m-thick cell-ECM intermediary [4]. The PCM is pivotal in transmitting biomechanical, biophysical and biological signals between the ECM and cells [5, 6], and is where the initial assembly of newly synthesized matrix molecules takes place [7, 8]. In healthy human cartilage, the modulus of PCM is \sim 50 kPa [9], much higher than that of the canonical hydrogel environment [1]. Despite being surrounded by a much stiffer matrix, residing chondrocytes can sustain their normal metabolic activities during development and maintenance *in vivo*. In osteoarthritis (OA), degeneration of the PCM is one of the earliest events upon disease initiation, leading to aberrant chondrocyte mechanotransduction, which contributes to the vicious loop of irreversible cartilage degeneration [9-11]. Understanding the biomechanical and biophysical characteristics of the native PCM will provide a much needed benchmark for engineered tissues to better recapitulate the native microniche of chondrocytes [12]. In addition, it is increasingly evident that changes in the ECM are the driving force of most human diseases, both congenital and acquired [13-15]. Knowledge about cartilage PCM could thus provide new insights into the roles of immediate cell micro-niche in other diseases as well [16-18].

In the past decades, there have been significant advances in understanding the roles of individual PCM biomolecules in cartilage health and disease [19], including type VI collagen [20-22], perlecan

[23-25], biglycan [26, 27] and matrilins [28-31]. Despite these efforts, the assembly, structure and mechanobiological functions of PCM remain poorly understood [5]. It is unclear how the native PCM maintains normal chondrocyte activities despite being much stiffer than the *in vitro* chondrogenic microenvironment. One distinctive feature of the native PCM is the preferential localization of specific proteoglycans [32]. In particular, aggrecan, the major proteoglycan of cartilage, is more concentrated in the PCM [33], where it undergoes faster turnover [34], and with newly synthesized aggrecan mainly localized there [35]. Aggrecan has a bottle-brush architecture, consisting of ~ 400 nm-long core protein decorated with > 100 densely packed, ~ 40 nm-long chondroitin sulfate glycosaminoglycan (CS-GAG) side chains. In cartilage, aggrecan contributes to > 90% of CS-GAGs and total fixed charges [19], and endows the matrix with its highly negatively charged environment [36]. Although the contribution of aggrecan to cartilage tissue-level biomechanics has been well documented [37], it is unclear whether or how aggrecan and its fixed negative charges impact the pericellular microenvironment and chondrocyte mechanosensing *in vivo*. It is also unclear how the structural integrity of aggrecan is maintained in the PCM, for that the primary assembly mechanism of aggrecan network, the link protein-assisted aggrecan-hyaluronan (HA) aggregation [38], does not fully address the diversity or changes in the retention of aggrecan at different development stages and disease states, or the preferential distribution of aggrecan in the PCM [35].

Decorin, a small leucine-rich proteoglycan, could play an important role in regulating the integrity of aggrecan in the PCM. Our recent studies showed that in decorin-null (*Dcn*^{-/-}) mice, loss of decorin leads to markedly reduced retention of aggrecan in the ECM, resulting in impaired cartilage biomechanical properties [39] and increased susceptibility to surgery-induced OA [40]. We further showed that decorin primarily functions as a “physical linker” to increase the molecular adhesion between aggrecan-aggrecan and aggrecan-collagen II fibrils, thereby strengthening the integration of aggrecan networks without directly affecting chondrocyte biology or aggrecan biosynthesis [39]. In

adult cartilage ECM, decorin and aggrecan are present in both the PCM and the territorial/interterritorial ECM (T/IT-ECM) that is further removed from cells [39]. We thus hypothesize that decorin is required for maintaining the integrity of aggrecan networks in the PCM. We tested this hypothesis by studying the nanostructural and micromechanical phenotype of *Dcn*^{-/-} cartilage PCM. We further queried if loss of decorin disrupts chondrocyte mechanotransduction by assessing the intracellular calcium signaling activities, $[Ca^{2+}]_i$, *in situ*, which are one of the earliest, fundamental cell responses to mechanical stimuli [41]. Then, by studying $[Ca^{2+}]_i$ signaling under enzymatic removal of CS-GAGs, we tested if the impact of decorin on chondrocytes is manifested through its regulation of aggrecan assembly in the PCM. Our findings suggest that the aggrecan-rich, highly negatively charged PCM microenvironment is essential for maintaining normal chondrocyte mechanosensitive activities, and decorin plays an important role in regulating the integrity of aggrecan in this critical microdomain.

RESULTS

***Dcn*^{-/-} cartilage pericellular matrix exhibits altered nanostructure and sGAG content.**

We first studied the impact of decorin loss on the morphology and structure of cartilage PCM. Specifically, we compared the distributions of key PCM biomolecules and the morphology of PCM between age-matched *Dcn*^{-/-} and wild-type (WT) mice *via* immunofluorescence (IF) staining. In WT cartilage, aggrecan and decorin were distributed throughout the ECM, as shown for mice at both 2 weeks and 3 months of age (Fig. 1a). The staining intensity of aggrecan was stronger in the pericellular domain, corroborating literature showing higher concentration of aggrecan in the PCM [33, 42, 43]. Similarly, the staining of decorin was also stronger in the pericellular domain, which was in alignment with the more intense staining of decorin reported in the middle zone of adult bovine cartilage [42] and adult rabbit knee cartilage [44]. To this end, additional imaging assays would help delineating the localization pattern of decorin in the PCM versus T/IT-ECM at different ages and within different tissue

regions. In addition, we imaged the three canonical biomarkers of cartilage PCM, collagen VI, perlecan and biglycan. All three molecules were found to localized in the PCM in both WT and *Dcn*^{-/-} cartilage at 2 weeks of age (Fig. 1b).

Applying immunolabeling of collagen VI to unfixed cartilage cryo-sections, we estimated the thickness of PCM in WT and *Dcn*^{-/-} cartilage at 3 days (newborn), 2 weeks (immature) and 3 months (adult) of ages (Fig. 2a,b). We also calculated the areas occupied by cells, PCM and T/IT-ECM on the sections, which approximately correspond to the volume proportions of the three domains (Fig. 2c). During maturation, the thickness of cartilage PCM, as well as volume proportions of the cell and PCM, decreased gradually, while the proportion of the T/IT-ECM increased (Fig. 2c, Table S1). These results illustrate that during post-natal growth, cartilage evolves from a highly cellularized, PCM-rich soft composite to a stiffer tissue that is more dominated by the T/IT-ECM, which is directly responsible for its specialized biomechanical functions at the tissue level.

In *Dcn*^{-/-} cartilage, we did not observe marked up-regulation or altered distribution of collagen VI, perlecan or biglycan (Fig. 1b). We also did not detect any appreciable differences in the thickness of PCM (Fig. 2b), or the volume proportions of cell, PCM and T/IT-ECM domains (Fig. 2c). This suggests that with the loss of decorin, the PCM retains its compositional and morphological distinction from the T/IT-ECM, and PCM-specific molecules are not substantially up-regulated to compensate for the loss of decorin. However, with the loss of decorin, the staining of aggrecan protein core and sGAGs were reduced in both the PCM and T/IT-ECM at 2 weeks and 3 months of age (Fig. 1a). This reduction of aggrecan is consistent with our recent observation that *Dcn*^{-/-} cartilage exhibits decreased aggrecan and sGAG content at the tissue level [39]. Thus, decorin plays a crucial role in regulating the structural integrity of aggrecan network assembly not only at the tissue level, but also in the pericellular matrix at the microscale.

Next, given that decorin can bind to collagen II fibril surfaces [45], we tested if loss of decorin alters the nanostructure of collagen fibrillar network in the PCM. As measured by TEM on cartilage from 3-month-old mice, for both genotypes, the PCM consists of significantly thinner fibrils relative to the T/IT-ECM (Fig. 2d, Table S2, $p < 0.0001$). In comparison to the WT, the PCM of $Dcn^{-/-}$ cartilage showed a mild increase in average collagen fibril diameter, d_{col} (Fig. 2e) but a salient increase in fibril heterogeneity (Fig. 2f). This observation is also consistent with our previous study reporting that the collagen fibrils in $Dcn^{-/-}$ cartilage T/IT-ECM showed no appreciable changes in average d_{col} , but a substantial increase in heterogeneity (Table S2). Taken together, loss of decorin did not alter the morphology or compositional distinction of cartilage PCM, but significantly reduced the aggrecan content therein, and had a minor effect on collagen fibrillar nanostructure.

$Dcn^{-/-}$ cartilage pericellular matrix develops reduced modulus during post-natal growth.

To determine if loss of decorin would affect the micromodulus of PCM, we applied the IF-guided AFM-nanomechanical mapping [10] on fresh, 6- μm -thick, unfixed sagittal cryo-sections of tibial cartilage prepared *via* the Kawamoto's film-assisted cryo-sectioning method (Fig. 3a) [46]. Guided by the IF-labelled images of collagen VI, we separated the micromoduli of the PCM and T/IT-ECM, and excluded the values corresponding to cell remnants (Fig. 3b). In WT cartilage, the modulus of PCM was significantly lower than that of the T/IT-ECM at all tested ages (Fig. 3b,c, Table S3). This suggests that as early as 3 days of age, the PCM has become distinct from the tissue bulk, providing chondrocytes with a specialized micromechanical niche that persists throughout post-natal growth and maintenance. This salient micromechanical heterogeneity is consistent with previous findings in porcine [47], human [9] and murine [10, 48] cartilage. From newborn to adult ages, the moduli of both PCM and T/IT-ECM increased significantly, e.g., for the PCM, from 0.058 ± 0.005 MPa (mean \pm 95% CI, $n = 5$) at 3 days of age to 0.285 ± 0.019 MPa at 2 weeks to 0.907 ± 0.056 MPa at 3 months (Fig. 3c), confirming the expected matrix stiffening with skeletal maturation [49].

In newborn mice, loss of decorin did not significantly alter the modulus of PCM (0.059 ± 0.018 MPa for $Dcn^{-/-}$ mice, $p = 0.974$ versus WT), indicating that decorin does not play a critical role in the embryonic development of cartilage matrix. In contrast, at 2 weeks of age, the modulus of $Dcn^{-/-}$ PCM was significantly reduced (0.212 ± 0.048 MPa) in comparison to WT ($26 \pm 10\%$ lower, $p = 0.001$), which became more substantial by 3 months of age (0.252 ± 0.072 MPa, $72 \pm 13\%$ lower, $p < 0.0001$). Also, in $Dcn^{-/-}$ mice, from 2 weeks to 3 months of age, the maturation-associated stiffening effect was absent for the PCM ($p = 0.167$). Similarly, the modulus of T/IT-ECM in $Dcn^{-/-}$ cartilage was also significantly reduced at 2 weeks ($23 \pm 6\%$) and 3 months ($72 \pm 4\%$) of ages, but not at 3 days of age (Fig. 3c, Table S3). This observation is consistent with our recent finding at the tissue level, in which, the loss of decorin leads to reduced cartilage modulus at more than 1 week of age [39]. Taken together, the marked impairment of PCM micromechanics and lack of maturation-associated stiffening in $Dcn^{-/-}$ cartilage underscore that decorin is indispensable for the establishment of cartilage PCM during postnatal growth.

$Dcn^{-/-}$ chondrocytes exhibit decreased intracellular $[Ca^{2+}]_i$ responses *in situ*.

Next, we tested if the impaired PCM, as a result of decorin loss, disrupts chondrocyte mechanotransduction. To directly connect the phenotype of native cartilage PCM with the mechanosensing of chondrocytes *in situ*, we studied the intracellular calcium signaling, $[Ca^{2+}]_i$, activities of freshly dissected tibia cartilage explants in both physiological (isotonic) and osmotically instigated (hypo- and hypertonic) Dulbecco's Modified Eagle Medium (DMEM). For both genotypes, we observed spontaneous $[Ca^{2+}]_i$ oscillations at all three tested ages, from which, we extracted the temporal $[Ca^{2+}]_i$ parameters, including the percentage of responding cells, $\%R_{cell}$, the total number of $[Ca^{2+}]_i$ peaks, n_{peak} , and the duration of averaged peaks, t_{peak} , from each responding cell over a 15 minute observation period (Fig. 4a,b). In isotonic DMEM, comparing the two genotypes, $Dcn^{-/-}$ chondrocytes had similar $[Ca^{2+}]_i$ responses to that of WT at 3 days of age, but showed significantly reduced activities (decreased $\%R_{cell}$,

n_{peak} , and increased t_{peak}) at both 2 weeks and 3 months of ages, with more pronounced changes at 3 months (Fig. 4c-e, Table S4). The two genotypes also exhibited differentiated responses to maturation. For WT cartilage, there was only a moderate decrease of $[\text{Ca}^{2+}]_i$ responses with age, where the 3-month group showed significantly lower n_{peak} and longer t_{peak} than the 3-day group, but no changes were found between other pairs for n_{peak} and t_{peak} , or among all three ages for $\%R_{\text{cell}}$. In contrast, $Dcn^{-/-}$ cartilage exhibited significantly decreased $[\text{Ca}^{2+}]_i$ responses between all age pairs and for all three parameters (Fig. 4c-e, Table S5).

Limited by the microscale dimension and irregular shape of murine knee cartilage, we were unable to directly apply well-defined compressive strains. Since the PCM is characterized by high proteoglycan concentration and consequently high negative fixed charge density [5], we applied osmotic stimuli instead. Under hypotonic stimuli, the electrical double layer (EDL) repulsion within the matrix is amplified [50]. At the same time, *in situ*, the stiffer surrounding PCM limits the spontaneous swelling response of chondrocytes to hypotonicity [51]. Thus, chondrocytes experience enhanced compressive stress, similar to the case of physiologic compression, which decreases the GAG-GAG spacing, resulting in enhanced EDL repulsion and osmotic pressure in the PCM. Conversely, hyper-osmotic stimuli lessen the EDL repulsion in the PCM, and reduce the compressive stress experienced by chondrocytes *in situ*.

For both genotypes at all three ages, chondrocyte $[\text{Ca}^{2+}]_i$ responses were significantly enhanced by hypo-osmolarity (increased $\%R_{\text{cell}}$, n_{peak} and/or shorter t_{peak}), and reduced by hyper-osmolarity (Table S6). Under these osmotically instigated stimuli, $Dcn^{-/-}$ chondrocytes again showed similar $[\text{Ca}^{2+}]_i$ responses as WT at 3 days of age, but decreased activities at 2 weeks and 3 months (Fig. 4c-e, Table S4). Furthermore, contrasts between the two genotypes were amplified by hypo-osmotic stimuli, as illustrated by a larger percentage of decrease in n_{peak} of $Dcn^{-/-}$ chondrocytes relative to WT (e.g., $59 \pm 4\%$ in hypotonic versus $51 \pm 3\%$ in isotonic DMEM at 3 months of age), and lessened by hyper-osmolarity ($42 \pm 9\%$ decrease). For t_{peak} , the differences were less pronounced, as $Dcn^{-/-}$ chondrocytes showed

similar degrees of increase relative to WT in hypotonic ($130 \pm 6\%$) and isotonic ($135 \pm 6\%$) conditions, and a lesser degree in hypertonic condition ($56 \pm 6\%$). Thus, chondrocyte $[\text{Ca}^{2+}]_i$ responses, as well as their extent of demotion in $Dcn^{-/-}$ cartilage, were both highly correlated with the degree of EDL repulsion and osmotic pressure present in the PCM.

Enzymatic removal of chondroitin sulfate suppresses chondrocyte $[\text{Ca}^{2+}]_i$ responses *in situ*.

To determine if aggrecan and its CS-GAG chains are a major determinant of chondrocyte mechanosensing *in situ*, we tested chondrocyte $[\text{Ca}^{2+}]_i$ signaling between the two genotypes after enzymatic removal of CS-GAGs from 2-week-old murine tibial cartilage. We employed a 12-hour chondroitinase ABC (C'ABC) treatment to induce maximal sGAG removal without significantly affecting cell viability [52]. In addition, using femoral head cartilage of 2-week-old mice, we assessed the impact of C'ABC treatment on sGAG content for both genotypes. In untreated, freshly dissected tissue, $Dcn^{-/-}$ cartilage ($3.9 \pm 0.4\%$ wet wt., $n = 4$) showed $22 \pm 8\%$ lower sGAG content relative to the WT ($5.0 \pm 0.7\%$, $p = 0.029$, Fig. 5a). Treatment of C'ABC resulted in $84 \pm 14\%$ and $80 \pm 13\%$ decrease in sGAG content in $Dcn^{-/-}$ ($0.7 \pm 0.2\%$) and WT ($1.0 \pm 0.3\%$) cartilage, respectively (Fig. 5a). After the treatment, the amount of residual sGAGs in $Dcn^{-/-}$ cartilage was $36 \pm 1\%$ lower than that in WT ($p = 0.029$, Fig. 5a).

For both genotypes, enzymatic removal of sGAGs did not alter $\%R_{\text{cell}}$ of $[\text{Ca}^{2+}]_i$ responses, but significantly reduced temporal characteristics, *e.g.*, lower n_{peak} in hypo- and isotonic DMEM, and longer t_{peak} in all three osmolarities (Fig. 5b-d, Tables S7 and S8). This confirms that CS-GAGs on aggrecan, and their associated fixed charges regulates chondrocyte mechanosensing *in situ*. As such, chondrocytes in $Dcn^{-/-}$ cartilage still exhibited decreased $[\text{Ca}^{2+}]_i$ responses in comparison to WT after the CS-GAG removal, as signified by lower n_{peak} in hypo- and isotonic conditions, and longer t_{peak} in all three osmolarities (Fig. 5b-d, Tables S7 and S8). This effect was more conspicuous when EDL repulsion was

amplified by hypo-osmolarity, as illustrated by the more pronounced differences in n_{peak} (Fig. 5c). Thus, the contrasts between C'ABC-treated and untreated groups for both genotypes, and between WT and $Dcn^{-/-}$ groups for both treatment conditions, both suggest that fixed charges in cartilage matrix, as endowed by aggrecan, contribute to maintaining the normal $[Ca^{2+}]_i$ activities of chondrocytes *in situ*.

DISCUSSION

Role of decorin in the integrity and micromechanobiology of cartilage PCM.

This study highlights a key role of decorin in regulating the integrity and mechanobiological functions of cartilage PCM, the immediate microenvironment of chondrocytes (Fig. 6). Previously, we found that decorin regulates the assembly of aggrecan networks and tissue-level biomechanics of cartilage ECM by increasing the molecular adhesion between aggrecan-aggrecan and aggrecan-collagen II fibrils [39]. This study shows that this regulatory role of decorin is essential for not only cartilage biomechanics at the tissue level, but also the integrity and mechanobiological functions of PCM at the microscale. In $Dcn^{-/-}$ cartilage, loss of decorin does not affect the compositional distinction between PCM and T/IT-ECM, the thickness of PCM or the PCM-to-T/IT-ECM volume ratio (Figs. 1b, 2a-c), but results in reduced aggrecan staining (Fig. 1a) and micromodulus (Fig. 3) of the PCM, as well as decreased chondrocyte $[Ca^{2+}]_i$ activities *in situ* (Fig. 4). Here, the loss of aggrecan and impairment of PCM micromechanics are resulted from decorin directly regulating the aggrecan network assembly, rather than a secondary effect from the moderate changes of collagen fibril nanostructure (Fig. 2) [39]. In other genetically modified mice deficient of key collagen fibrillar constituents, such as collagens IX [53], XI [54] and III [48], despite the presence of much more pronounced structural defects in collagen fibrils, the amount of aggrecan and sGAGs in cartilage appeared to be normal.

In comparison to the T/IT-ECM that is further-removed from chondrocytes, the PCM has thinner collagen fibrils (Table S2), which provides a greater surface-to-volume ratio for decorin to interact with.

This interaction could facilitate the physical connection between aggrecan and collagen fibrils through decorin, thereby enhancing the retention of aggrecan in the PCM (Fig. 6). Such mechanism could thus help explain why aggrecan is more concentrated in the PCM despite its ubiquitous presence throughout cartilage matrix. In addition, decorin binds to aggrecan through PCM-specific molecules including collagen VI and matrilin-1 [55, 56], which may further strengthen decorin-aggrecan interactions in the PCM. These interactions, however, may not be essential, for that neither *Col6a1*^{-/-} [21] nor matrilin-null murine cartilage (*Matn1*^{-/-} [28, 29], *Matn3*^{-/-} [30] and *Matn1-4*^{-/-} [31]) yielded the same phenotype of salient aggrecan reduction as in *Dcn*^{-/-} cartilage. Meanwhile, the lack of phenotype in newborn *Dcn*^{-/-} cartilage PCM (Fig. 3b,c) suggests that decorin is not required for initiating the aggrecan network assembly during embryonic development. However, during post-natal growth, the “physical linkage” provided by decorin becomes increasingly important, when cartilage experiences extensive joint loading, and the associated interstitial fluid flow could aggravate the diffusive loss of aggrecan in the absence of decorin and its stabilizing effect on aggrecan network.

We further showed that the integrity of aggrecan network in the PCM, as regulated by decorin, is required for normal mechanotransduction of chondrocytes. Chondrocytes are highly sensitive to their mechanical environment, and $[Ca^{2+}]_i$ activities are one of the earliest, fundamental events in their responses to mechanical stimuli [41]. Transmembrane ion channels, such as transient receptor potential vanilloid-4 (TRPV4) [57] and mechanosensitive ion channels Piezo1/2 [58], are activated when chondrocyte cell membrane experiences external stimuli under deformation or osmotic stress. These activities are critical in mediating cartilage homeostasis and disease pathogenesis [59]. *In situ*, their activation is regulated by the immediate cellular microniche, i.e., the PCM. In the PCM, aggrecan and its CS-GAGs provide strain shielding for chondrocytes, and couple mechanical loading with interstitial osmolarity [60]. Meanwhile, the negatively charged environment sequesters counter ions, providing the immediate extracellular Ca^{2+} sources to mediate the activation of ion channels [61]. Here, the decreased

chondrocyte $[Ca^{2+}]_i$ responses *in situ* under CS-GAG removal (Fig. 5) highlights the importance of PCM aggrecan in maintaining chondrocyte mechanotransduction. In alignment with this effect, in the absence of decorin, when the reduction of aggrecan and impairment of PCM micromechanics are amplified with maturation (Fig. 3), demotion of chondrocyte $[Ca^{2+}]_i$ responses also becomes increasingly pronounced (Fig. 4). These results together support an important role of decorin in regulating chondrocyte mechanotransduction *in vivo* by mediating its immediate microenvironment. To this end, while the exact biological pathways by which $[Ca^{2+}]_i$ activities influence downstream signaling are not fully understood, $[Ca^{2+}]_i$ activities have been shown to be positively correlated with chondrocyte anabolism [62], and demotion of $[Ca^{2+}]_i$ signaling is one of the earliest events preceding the onset of post-traumatic OA [10]. Therefore, although decorin appears not to directly influence chondrocyte biosynthesis in the absence of mechanical stimuli in both alginate [39] and explant [40] cultures, it is possible that, by regulating the integrity of the PCM, decorin could impact the mechanosensitive activities of chondrocytes, and thus, the establishment and homeostasis of cartilage matrix *in vivo* (Fig. 6).

Comparison to the activities of other PCM-specific molecules in cartilage.

This structural role of decorin is distinct from the known activities of other PCM-specific biomolecules. In the PCM, collagen VI forms a hexagonal beaded network, and is found to regulate PCM micromodulus, chondrocyte swelling, $[Ca^{2+}]_i$ signaling *in situ* [22], as well as integrin $\alpha 1\beta 1$ -mediated chondrocyte-matrix interactions [63]. However, loss of collagen VI does not alter the properties of T/IT-ECM [63], and leads to variable responses to OA in *Col6a1^{-/-}* mice [20-22], indicating its impact is largely limited to the integrity of PCM, rather than the ECM as a whole. In contrast, decorin impacts both the PCM and T/IT-ECM (Fig. 3), and loss of decorin aggravates cartilage fibrillation and degradation in OA [40], suggesting a more essential role of decorin in the overall health of cartilage. Perlecan is a heparan-sulfate proteoglycan that directly regulates cell surface mechanosensing [64] and activation of fibroblast growth factor-2 (FGF-2) [65]. Reduction of perlecan in *Hspg2^{+/+}* mice results in

impaired matrix development in embryonic joints [66]. Decorin, on the other hand, is not required for embryonic development, and only becomes more important during post-natal growth. Biglycan, another class I SLRP, is highly structurally homologous to decorin, but harbors two, instead of one, CS/DS-GAG chains near its N-terminus [67]. While decorin and biglycan have coordinated and compensatory activities in tendon [68, 69] and cornea [70], their roles in cartilage are distinct. The importance of biglycan to cartilage health is illustrated by accelerated spontaneous OA in *Bgn*^{-/-} mice [26, 27], while soluble biglycan in cartilage may have an adverse effect by evoking inflammation through toll-like receptor-4 (TLR-4) [71]. Unlike decorin, biglycan primarily plays biological roles in regulating chondrocyte signaling. The absence of biglycan in the T/IT-ECM of *Dcn*^{-/-} cartilage (Fig. 1b) also suggests that biglycan is not up-regulated to compensate for the loss of decorin, unlike the cases of tendon and cornea [68-70].

Comparison to other studies of *Dcn*^{-/-} murine cartilage.

Our finding that *Dcn*^{-/-} cartilage has lower micromodulus in both the PCM and T/IT-ECM than the WT control (Fig. 3) is different from the previous work by Gronau et al., which reported a higher modulus of *Dcn*^{-/-} cartilage [72]. We attribute such contrast to differences in sample preparation, storage, length scale and geometry of AFM indenters, as well as the data analysis methods used in these studies [39]. In Gronau et al., AFM-nanoindentation was performed on 30- μ m-thick cartilage cryo-sections using pyramidal tips (nominal radius $R \approx 20$ nm, half open angle $\approx 20^\circ$), and the stiffness values are suggested to represent local micromechanics of individual ECM proteoglycans and collagen fibrils [73]. In this study, AFM-nanomechanical mapping was performed using microspherical indenter tips ($R \approx 2.25$ μ m) with a maximum depth of $D_{\max} \approx 0.5$ μ m, yielding a ≈ 1.4 μ m effective tip-sample contact radius, or ≈ 6.3 μ m² contact area. Given that each aggrecan molecule consists of a ≈ 400 nm-long core protein with ≈ 40 nm-long CS-GAGs [37], the micromodulus of PCM reflects the integrated response of a few aggrecan molecules, collagen fibrils (\approx 30-80 diameter [39]) and other minor matrix constituents

at the microscale, rather than that of individual matrix molecules. In addition, guided by the immunolabelling of collagen VI, we partitioned the micromodulus map into three distinct domains, i.e., the T/IT-ECM, PCM and cell remnants. As discussed in our recent study, this partition is necessary for accurately assessing the local micromodulus of biological tissues with high cell density and spatial heterogeneity [10]. For example, moduli measured on domains corresponding to chondrocytes represent cytoplasma and nucleus remnants damaged during cryo-sectioning, and inclusion of these data would substantially underestimate the micromodulus of cartilage matrix [10]. With this IF-guided partitioning, for both WT and *Dcn*^{-/-} cartilage, the micromodulus of T/IT-ECM measured here (Table S3) are in quantitative agreement with the tissue-level modulus reported in our previous study (WT: 0.22 ± 0.08 MPa, 0.60 ± 0.06 MPa, 1.45 ± 0.21 MPa, *Dcn*^{-/-}: 0.19 ± 0.05 MPa, 0.39 ± 0.05 MPa, 0.46 ± 0.06 MPa at 3 days, 2 weeks and 3 months of ages, respectively) [39]. Furthermore, the micromodulus of 3-month-old WT cartilage T/IT-ECM measured here (1.54 ± 0.10 MPa) is also similar to the tissue-level modulus of young adult, healthy murine cartilage previously measured by AFM-nanoindentation [74-77] and instrumented microindentation [20, 78, 79], which are all in the range of ~ 1 -2 MPa.

Potential application of decorin as a target for cartilage regeneration.

In cartilage tissue engineering, biosynthesis of aggrecan and collagen II is often elevated by external biochemical and/or biophysical cues [80]. Given the mechanosensitive nature of chondrocytes, dynamic loading is one most commonly used biomechanical stimulus [81]. In this regard, both partially preserved native PCM or pre-deposited neo-PCM can help transmit mechanical signals, enhancing chondrocyte anabolic responses to dynamic loading [82]. On the other hand, dynamic loading and associated interstitial fluid flow often aggravate the loss of newly synthesized aggrecan from developing neo-PCM, resulting in impaired tissue assembly [83]. This represents a major challenge in mesenchymal stem cell (MSC)-based cartilage regeneration, for that chondrogenically differentiated MSCs are less capable of retaining newly synthesized aggrecan relative to primary chondrocytes [84]. According to

this study, decorin has the potential to enhance aggrecan retention in the neo-PCM formed under dynamic loading for both cell types [85]. Furthermore, transforming growth factor (TGF- β) is one most commonly used biochemical cue to elevate chondrocyte anabolism [86]. While decorin is shown to sequester TGF- β signaling through binding to TGF- β in other tissues [87], according to our recent work, decorin does not directly impact chondrocyte response of TGF- β stimuli when cultured in alginate [39]. Therefore, modulation of decorin activities *in vitro* is a promising path for improving the assembly of cartilage neo-matrix and harnessing chondrocyte mechanotransduction without having a detrimental impact on chondrocyte responses to biochemical or biomechanical cues.

In murine cartilage, the modulus of PCM is up to ~ 1 MPa (Fig. 2), which is more than ten-fold stiffer than the soft environment required for chondrocyte culture *in vitro* [1]. In comparison to various biopolymer systems, including hyaluronan-based hydrogels [88], one distinctive biophysical feature of the native PCM is the high concentration of aggrecan and associated high density of negative fixed charges. As shown here, this negatively charged environment is required for maintaining chondrocyte mechanosensing *in situ* (Fig. 5). Thus, if we can recreate the osmo-microenvironment *in vitro*, either using native aggrecan or biomimetic molecules, there is a path for us to restore the high stiffness of native cartilage while maintaining normal chondrocyte mechanotransduction [89, 90]. In this process, decorin could be a key player.

Limitations and outlook.

This study has several limitations. First, in *Dcn*^{-/-} mice, both the PCM and T/IT-ECM are impaired at the same time. It is possible that the decreased $[Ca^{2+}]_i$ signaling in *Dcn*^{-/-} chondrocytes can be partially attributed to the altered T/IT-ECM. However, given the immediate contact of PCM with cells, we expect the integrity of PCM to have a more direct impact. To address this, our ongoing studies aim to elucidate the role of decorin in regulating the mechanosensing of chondrons extracted from native

cartilage and chondrocytes integrated with neo-PCM, which will eliminate any secondary effects of the T/IT-ECM. We will assess how the modulation of decorin gene expression and/or exogenous decorin availability alter chondrocyte biosynthesis and neo-matrix assembly when cultured in hydrogels under applied oscillatory dynamic compression using the bioreactor equipped with a compressive loading device [91]. Second, to maintain cell viability, we did not completely remove sGAGs from cartilage explants (Fig. 5). We thus cannot conclude if the impact of decorin on chondrocyte $[Ca^{2+}]_i$ activities is due to its regulation of aggrecan integrity or other mechanisms. Given the wide interactome of decorin with other cytokines, growth factors and receptors [92-95], it is possible for decorin to also regulate chondrocyte signaling through other biological activities. For example, soluble decorin and its core protein has been shown to mediate the intracellular calcium levels of squamous carcinoma cells by regulating epidermal growth factor receptors (EGFRs) [96, 97]. We therefore cannot rule out the possibility that decorin regulates chondrocyte $[Ca^{2+}]_i$ through mechanisms other than mediating the local fixed charge density of PCM, which may contribute to the observation that *Dcn*^{-/-} chondrocytes still show reduced $[Ca^{2+}]_i$ activities relative to WT even after most CS-GAGs have been removed (Fig. 5).

CONCLUSIONS

In summary, this study shows that decorin, a small leucine-rich proteoglycan, functions as an important regulator of the micromechanics and mechanobiological function of cartilage pericellular matrix. *In vivo*, as chondrocyte resides in an aggrecan-rich, highly negative charged osmo-microenvironment, decorin influences chondrocyte mechanotransduction mainly through mediating the integrity of aggrecan in the PCM. These findings extend our recent discoveries on decorin activities in cartilage tissue-level biomechanics and OA pathogenesis, and highlight decorin as an indispensable constituent of cartilage PCM. Based on this understanding, modulation of decorin has the potential to enhance the retention and assembly of aggrecan in the neo-matrix of regenerative cartilage, thereby improving the quality of engineered cartilage while maintaining cell chondrogenic phenotype.

METHODS

Animal model.

Decorin-null (*Dcn*^{-/-}) mice in the C57BL/6 strain were generated as previously described [98], and were housed in the Calhoun animal facility at Drexel University. Tissues were harvested from WT and *Dcn*^{-/-} mice at newborn (3-day old), immature (2-week old) and adult (3-month old) ages from littermates of *Dcn*^{+/+} breeders. Both male and female mice were included, for that we did not observe sex-associated variations in the phenotype of *Dcn*^{-/-} cartilage [39]. All animal work was approved by the Institutional Animal Care and Use Committee (IACUC) at Drexel University.

Immunofluorescence imaging.

Whole joints were harvested from WT and *Dcn*^{-/-} mice, fixed in 4% paraformaldehyde, and then, decalcified in 10% EDTA for 7 days for joints at 2 weeks and 3 months of ages, respectively ($n = 4$ for each genotype at each age). Samples were embedded in paraffin and serial 6- μ m-thick sagittal sections were cut across the joint. Following established procedures [99], sections were incubated with the primary antibodies for aggrecan (AB1031, MilliporeSigma, Burlington, MA, 1:100), decorin (LF-114, Kerafast, Boston, MA, 1:100), collagen VI (70R-CR009X, Fitzgerald, Acton, MA, 1:200 dilution), perlecan (A7L6, Santa Cruz Biotech, Dallas, TX, 1:200) and biglycan (ABT271, MilliporeSigma, 1:100) overnight in 4°C. Sections were then incubated with secondary antibodies directed against the primary antibodies for collagen VI (28903, Rockland, Pottstown, PA, 1:200), perlecan (A11006, Invitrogen, Carlsbad, CA, 1:200), as well as for aggrecan, decorin and biglycan (RE234142, Invitrogen, 1:500), respectively, for 1hr at room temperature. All imaging was performed on an Olympus FV1000 laser scanning microscope (Olympus, Center Valley, PA).

Transmission electron microscopy.

Transmission electron microscopy (TEM) was applied to the cross-sections of 3-month-old murine cartilage, following established procedures [100]. Thin cross-sections (≈ 90 nm thick) were prepared on freshly dissected condyles fixed with Karnovsky's fixative for 15 min, followed by 1% osmium tetroxide for 1 hr, dehydrated in graded ethanol solutions, infiltrated and embedded in a mixture of EMbed 812, nadic methyl anhydride, dodecenylsuccinic anhydride and DMP-30 (EM Sciences, Fort Washington, PA), and polymerized at 60°C overnight, as described previously [39]. High resolution images were taken in the pericellular regions (< 2 μ m from cell surface) of uncalcified cartilage middle深深 zone at 80 kV using a JEOL 1400 TEM (JEOL, Tokyo, Japan). For each region, collagen fibril diameter was measured in ImageJ ($\geq 1,400$ fibrils from $n = 4$ animals for each genotype).

Immunofluorescence-guided AFM nanomechanical mapping.

Cryo-sections of fresh, unfixed tibia cartilage at ≈ 6 μ m-thickness in the sagittal plane were prepared in the optimal cutting temperature (OCT) media using the Kawamoto's film-assisted method [46], as described previously ($n = 5$ for each group) [10]. Cryo-sections were fluorescently labeled by cartilage PCM biomarker, collagen VI [4] (primary antibody: 70R-CR009X, Fitzgerald, 1:50; secondary antibody: goat anti-rabbit IgG, Lot 28903, Rockland, 1:200, for 20 minutes each). Samples were then tested using the Total Internal Reflection Fluorescence (TIRF) guided-AFM (MFP-3D, Asylum Research, Goleta, CA) in PBS with protease inhibitors (Pierce A32963, ThermoFisher, Waltham, MA). Within each 20×20 μ m 2 region of interest (ROI) with well-defined, ring-shaped PCM terrains [47], AFM nanomechanical mapping was performed in a 40×40 grid (1,600 indents) using polystyrene microspherical tips ($R \approx 2.25$ μ m, nominal $k \approx 0.6$ N/m, HQ:NSC36/tipless/Cr-Au, cantilever C, NanoAndMore, Watsonville, CA) up to ≈ 100 nN maximum indentation force at 10 μ m/s effective indentation depth rate (≥ 3 -4 ROIs for each joint). The effective indentation modulus, E_{ind} , was calculated by fitting the entire loading portion of the indentation force-depth (F - D) curve to the finite thickness-corrected Hertz model (Fig. 3b) [101]. The modulus of Kawamoto's film was assumed to be

infinite, as it was $> 10 \times$ higher than that of cartilage ($\approx 17.0 \pm 4.2$ MPa) [10]. Using corresponding IF images of collagen VI, we partitioned each map into three domains: the PCM, T/IT-ECM, and the domain corresponding to cellular remnants using a custom MATLAB (MathWorks, Natick, MA) code. We then analyzed the moduli of PCM and T/IT-ECM separately and excluded values corresponding to cell remnants.

Intracellular $[\text{Ca}^{2+}]_i$ signaling under osmotic stimulation.

At each age, for additional mice ($n = 4$ for each group), we labeled cells within the tibia with intracellular calcium indicator Ca-520TM AM (15 μM , AAT Bioquest, Sunnyvale, CA) in isotonic DMEM at 37°C for 1 hr, and then, gently washed three times with DMEM. Time-series of confocal images were taken at 37°C on the same group of cells every 2 seconds for up to 15 min using a LSM 700 laser scanning confocal microscope with a 20 \times objective (Zeiss, Oberkochen, Germany) in hypotonic (165 mOsm, ionic strength (IS) = 0.075 M), isotonic (330 mOsm, IS = 0.15 M), and hypertonic (550 mOsm, IS = 0.23 M) DMEMs with protease inhibitors (Pierce 88266, ThermoFisher). For each genotype, age and osmolarity, 50-60 chondrocytes in each sample were analyzed, following established procedures [102]. The pattern of $[\text{Ca}^{2+}]_i$ oscillation in each cell was characterized by the intensity of the fluorescent signal and its transient behavior. A responsive cell was considered as any cell in which the magnitude of the peak signal exceeded four times the maximum fluctuation of the baseline signal. The percentage of responding cells, $\%R_{\text{cell}}$, was calculated by determining the proportion of responsive cells relative to the total cell number within a region of interest. For every cell that was responsive, the total number of $[\text{Ca}^{2+}]_i$ peaks, n_{peak} , was counted during the 15-minute observation period, and the average duration of peaks, t_{peak} , was extracted from each $[\text{Ca}^{2+}]_i$ transient of responding cells.

Intracellular $[\text{Ca}^{2+}]_i$ signaling with the enzymatic removal of sGAGs.

Additional tibia joints were harvested from 2-week-old WT and *Dcn*^{-/-} mice ($n = 4$ for each group), and treated with 0.5 units/mL of protease-free chondroitinase ABC (C'ABC, C3667, Sigma-Aldrich) for 12 hours, with the contralateral knee cultured in serum-free DMEM for the same duration as the untreated control [52]. Samples were then labeled with Ca-520TM AM and time series images were obtained and analyzed at three different osmolarities, as described in the previous section. To estimate the degree of sGAG depletion, we repeated the same C'ABC treatment process on femoral head cartilage explants extracted from 2-week-old mice ($n = 4$ for each group), and measured the amount of sGAGs in the explants for both C'ABC-treated and untreated control using the standard dimethylmethylene blue (DMMB) dye assay [103].

Statistical analysis.

Linear statistical models were applied to analyze all quantitative outcomes using the R package lme4 (version 1.1-19) [104]. For continuous dependent variables including E_{ind} , t_{peak} , sGAG content, PCM thickness, as well as the area proportions of cell, PCM and T/IT-ECM domains, the linear mixed effect model was applied. For non-continuous variables, the generalized linear model was applied to n_{peak} (count) with the Poisson family, and to $\%R_{\text{cell}}$ (binary) with the binomial family, respectively. In these tests, genotype (WT versus *Dcn*^{-/-}), age (3 days to 3 months), treatment type (untreated versus C'ABC treated), tissue region (PCM versus T/IT-ECM) and osmolarity condition (hypo-, iso- and hypertonic) were treated as fixed effect factors when applicable, with interaction terms between genotype and age, or between genotype and treatment type, while the individual animal effect was treated as a randomized factor. Prior to the test, likelihood ratio test was applied to the data to determine the choice of two covariance structures, unstructured versus compound symmetry. For all the variables, we found significant interactions between genotype and age ($p < 0.0001$). In contrast, for sGAG content and $[\text{Ca}^{2+}]_i$ signaling outcomes, we did not find significant interactions between genotype and treatment conditions ($p > 0.10$). Holm-Bonferroni family-wise error correction was applied to adjust for multiple

contrasts when testing the effect of genotype at each age or for each treatment type, or the effect of treatment for each genotype, in which, each region or osmolarity condition was analyzed separately. Within each genotype, Tukey-Kramer post-doc multiple comparison was applied to perform pair-wise comparisons among the tested ages, osmolarity conditions or tissue regions. For collagen fibril diameter data, since > 200 measurements were repeated for each group, according to the central limit theorem, unpaired two-sample z -test was used to compare the average values of d_{col} between the two genotypes, and two-sample F -test was applied to compare the variances of d_{col} , followed by Holm-Bonferroni family-wise error correction. Statistical outcomes on the effects of genotype, age and treatment were summarized in Tables S1-S8. In all the tests, the significance level was set at $\alpha = 0.05$, and all the p -values have been adjusted for family-wise type I errors.

AUTHOR CONTRIBUTIONS

Conceptualization, L.H.; Supervision, L.H.; Data Collection and Analysis, D.R.C., B.H., Y.Z., C.W., S.M.A., P.C., B.K., S.-J.H. and D.K.; Data Interpretation, D.R.C., B.H., C.W., M.E.-I., X.L.L., R.V.I., D.E.B., R.L.M. and L.H.; Writing, B.H., C.W., R.V.I., L.H.; Funding Acquisition, L.H. All authors intellectually contributed and provided approval for publication.

DECARATIONS OF INTEREST

None.

ACKNOWLEDGEMENTS

This work was supported by the National Institutes of Health (NIH) Grant AR074490 to LH, the National Science Foundation (NSF) Grant CMMI-1662544 and CMMI-1751898 to LH, Drexel Interdisciplinary Collaboration and Research Enterprise (iCARE) for Healthcare by the U.S. Department of Education's Graduate Assistance in Areas of National Need (GAANN) Program to DRC, as well as NIH Grant P30 AR069619 to the Penn Center for Musculoskeletal Disorders (PCMD). The IF-guided

AFM nanomechanical mapping was carried out using the TIRF MFP-3D at the Singh Center for Nanotechnology at the University of Pennsylvania, part of the National Nanotechnology Coordinated Infrastructure Program, which is supported by the NSF Grant NNCI-1542153.

ABBREVIATIONS USED

AFM, atomic force microscopy; CS, chondroitin sulfate; C'ABC, chondroitinase ABC; DMEM, Dulbecco's Modified Eagle Medium; DMMB, dimethylmethylen blue; DS, dermatan sulfate; ECM, extracellular matrix; EDL, electrical double layer; EGFR, epidermal growth factor receptor; GAG, glycosaminoglycan; HA, hyaluronan; IF, immunofluorescence; IS, ionic strength; MFP, molecular force probe; MSC, mesenchymal stem cell; OA, osteoarthritis; PBS, phosphate buffered saline; PCM, pericellular matrix; ROI, region of interest; sGAG, sulfated glycosaminoglycan; T/IT-ECM, territorial/interterritorial extracellular matrix; TEM, transmission electron microscopy; TIRF, total internal reflection fluorescence; TLR, toll-like receptor; WT, wild-type.

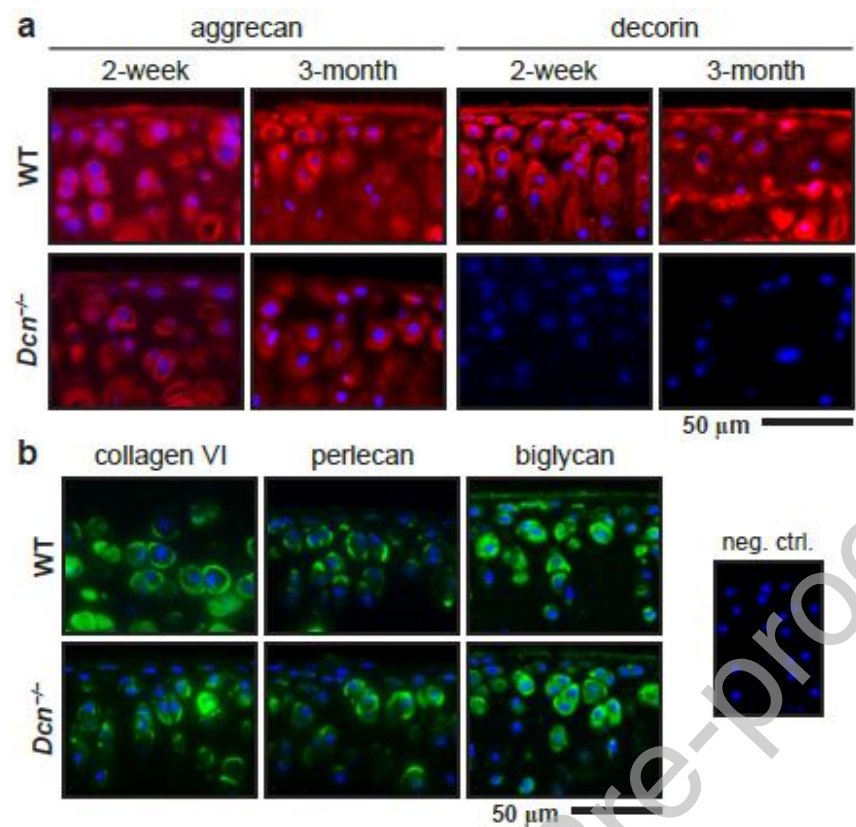
FIGURE CAPTIONS

Figure 1. Distribution of extracellular matrix biomolecules in wild-type (WT) and decorin-null (*Dcn*^{-/-}) cartilage *via* immunofluorescence (IF) imaging. a) IF images illustrate the reduced staining of aggrecan core protein and the absence of decorin in *Dcn*^{-/-} cartilage at 2 weeks and 3 months of ages. b) IF images show similar distribution of pericellular matrix (PCM) biomarkers, type VI collagen, perlecan and biglycan, in WT and *Dcn*^{-/-} cartilage at 2 weeks of age (blue: DAPI; shown together was the negative control).

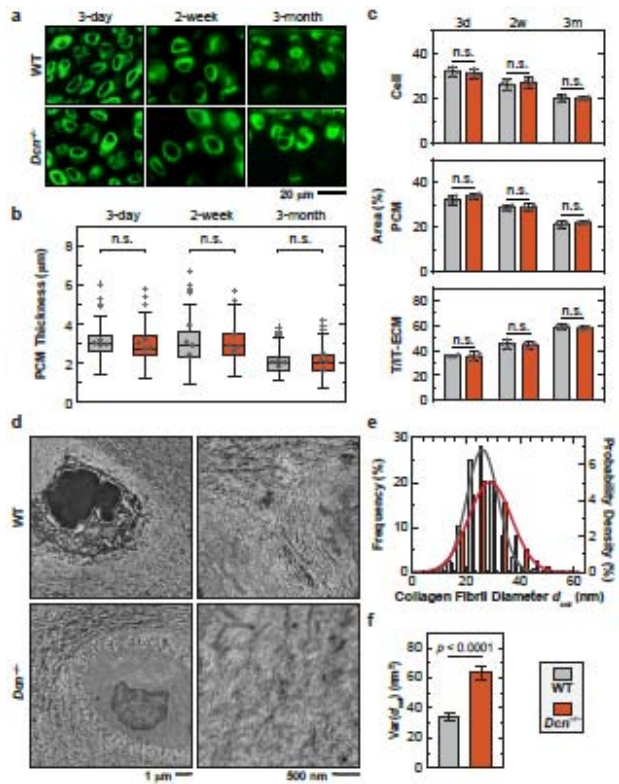


Figure 2. Decorin-null (*Dcn*^{-/-}) cartilage develops normal PCM morphology and moderate changes of collagen fibrillar nanostructure in the PCM. a) Representative immunofluorescence (IF) images on fresh, unfixed cartilage cryo-sections immunolabeled with type VI collagen at 3 days, 2 weeks and 3 months of ages. b) Box-and-whisker plot of the distribution of cartilage PCM thickness (≥ 120 cells from $n = 4$ animals for each genotype). c) Comparison of the proportions of areas occupied by the cell, PCM and T/IT-ECM in WT and *Dcn*^{-/-} cartilage ($n = 4$). See Table S1 for the complete list of descriptive statistics and adjusted p -values. d) Representative TEM images of collagen fibril structure on the sagittal sections of 3-month-old wild-type (WT) and *Dcn*^{-/-} cartilage PCM. e) Histogram of fibril diameter distribution ($> 1,400$ fibrils from $n = 4$ animals). Shown together were the normal distribution, $N(\mu, \sigma^2)$, fits to fibril diameters (for each fit, values of μ and σ correspond to the mean and standard deviation of fibril diameters shown in Table S2). f) Comparison of fibril diameter heterogeneity (variance) between the two genotypes (mean \pm 95% CI).

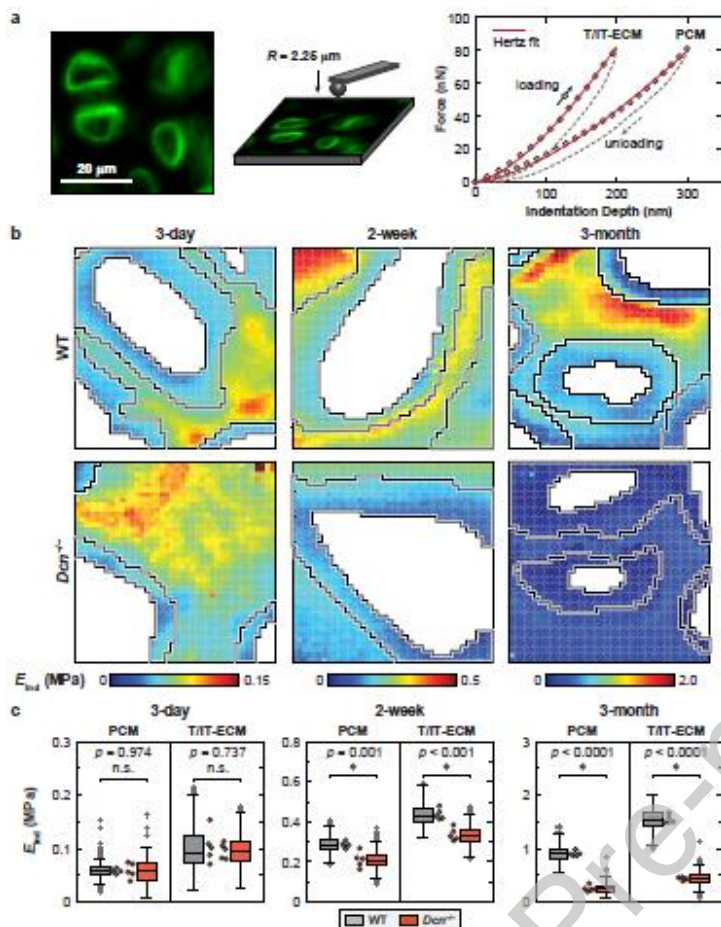


Figure 3. Decorin-null ($Dcn^{-/-}$) cartilage exhibits reduced micromodulus in the PCM and T/IT-ECM. a) Left panel: Schematic illustration of immunofluorescence (IF)-guided AFM nanomechanical mapping on the cryo-section of 2-week-old wild-type (WT) murine cartilage using a microspherical tip ($R \approx 2.25 \mu\text{m}$); the PCM is immunolabeled with collagen VI. Right panel: Two representative indentation force versus depth (F - D) curves obtained on the 2-week-old WT cartilage cryo-section (measured in PBS, 10 $\mu\text{m}/\text{s}$ rate), solid line: finite thickness-corrected Hertz model fit to the entire loading portion of the F - D curve. b) Representative indentation modulus maps of the PCM and T/IT-ECM partitioned for WT and $Dcn^{-/-}$ cartilage at 3 days, 2 weeks and 3 months of ages. Moduli corresponding to cell remnants were removed (white voids). c) Box-and-whisker plots of the PCM and T/IT-ECM micromodulus for WT versus $Dcn^{-/-}$ cartilage at each age ($> 1,100$ locations for each region, $n = 5$ animals). Each circle represents the average modulus of one animal, *: $p < 0.05$ between WT and $Dcn^{-/-}$ cartilage; n.s.: not significant. See Table S3 for the complete list of descriptive statistics and adjusted p -values.

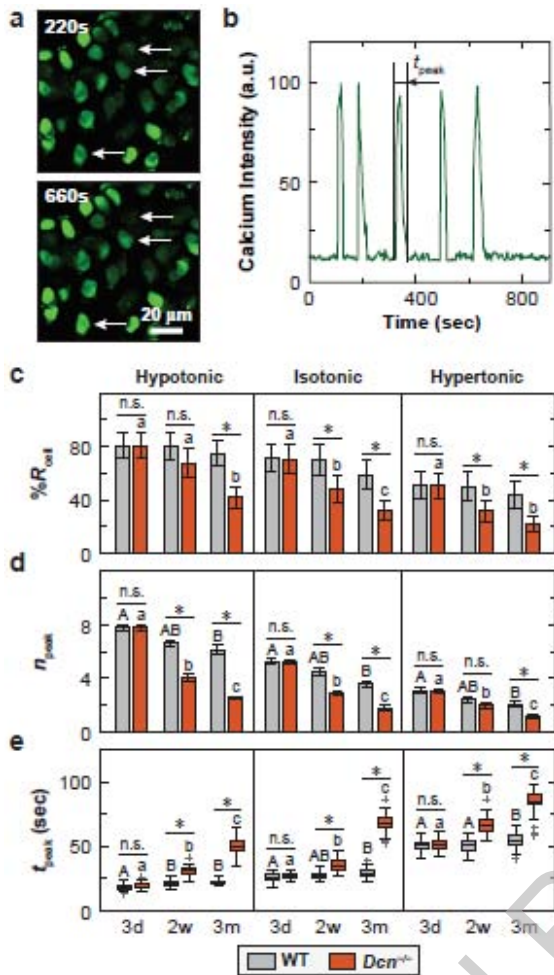


Figure 4. Decorin-null ($Dcn^{-/-}$) chondrocytes exhibit decreased chondrocyte intracellular Ca^{2+} activities *in situ*. a) Representative confocal images of $[\text{Ca}^{2+}]_i$ signaling in isotonic DMEM for 2-week-old wild-type (WT) cartilage explants. Chondrocytes were labeled with Ca-520TM AM and time series images were recorded using a confocal microscope with a 20 \times objective submerged in DMEM at 37 °C. b) Representative $[\text{Ca}^{2+}]_i$ oscillation intensity curve of a single cell over a 15-min time frame illustrating the definition of t_{peak} , the duration of each peak. c-e) Comparison of $[\text{Ca}^{2+}]_i$ signaling characteristics between WT and $Dcn^{-/-}$ chondrocytes at each age and osmolarity: c) percentage of responding cells, $\%R_{\text{cell}}$ (mean \pm 95% CI), d) number of peaks within the 15-min testing time frame, n_{peak} (mean \pm 95% CI), e) duration of each peak, t_{peak} (box-and-whisker plot). Data represent > 40 responding cells pooled from $n = 4$ animals for each group. *: $p < 0.05$ between genotypes; n.s.: not significant. For longitudinal comparisons, in WT cartilage, there was no significant difference among all three ages for $\%R_{\text{cell}}$ in all three osmolarities. Different letters indicate significant differences between ages within each genotype. See Tables S4-S6 for the complete list of descriptive statistics and adjusted p -values.

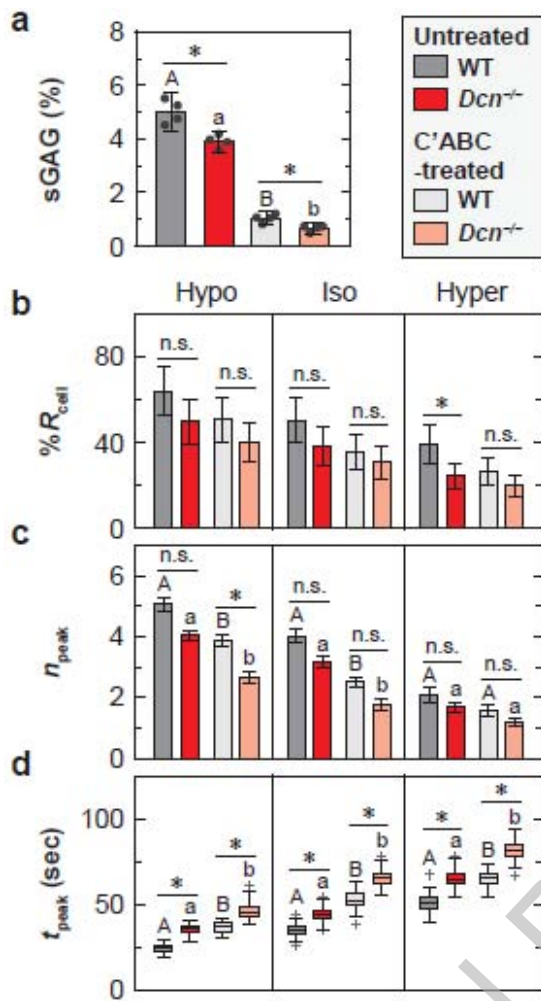


Figure 5. Impact of enzymatic removal of chondroitin-sulfate glycosaminoglycans (CS-GAGs) on chondrocyte intracellular Ca^{2+} activities *in situ*. a) Comparison of the amount of sGAGs in chondroitinase ABC (C'ABC)-treated and untreated cartilage explants from wild-type (WT) and decorin-null ($Dcn^{-/-}$) mice subjected to 12 hours C'ABC treatment at 37°C. b-d) Comparison of $[\text{Ca}^{2+}]_i$ signaling characteristics between the untreated and C'ABC-treated cartilage at 2 weeks of age in DMEM: b) percentage of responding cells, $\%R_{\text{cell}}$ (mean \pm 95% CI), c) number of peaks within the 15-min testing timeframe, n_{peak} (mean \pm 95% CI), and d) duration of each peak, t_{peak} (box-and-whisker plot). Data represent > 40 responding cells pooled from $n = 4$ animals for each group. *: $p < 0.05$ between genotype within each treatment group (n.s.: not significant). For both WT and $Dcn^{-/-}$ cartilage, there was no significant difference between treatment groups for $\%R_{\text{cell}}$ in all three osmolarities. Different letters indicate significant differences between treatment groups within each genotype. See Tables S7-S8 for the complete list of descriptive statistics and adjusted p -values.

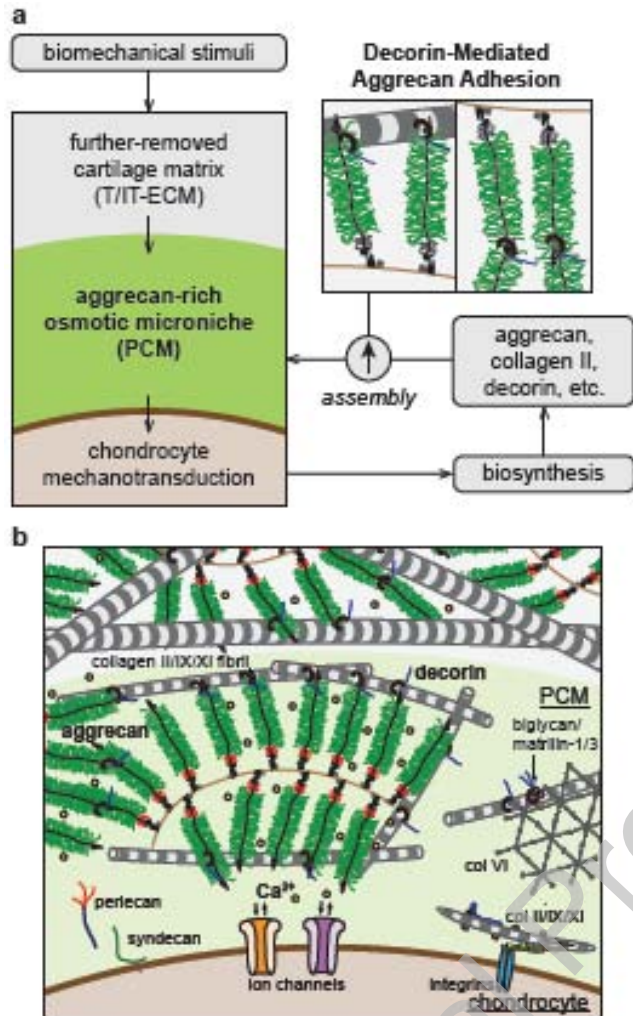


Figure 6. Schematic illustration of the working hypothesis on the structural role of decorin in cartilage pericellular matrix (PCM). a) Decorin regulates the structural integrity of PCM by mediating the molecular adhesion of aggrecan-aggrecan and aggrecan-collagen II fibrils therein. As a result, decorin regulates the PCM-mediated transmission of biomechanical stimuli from the extracellular matrix to chondrocytes, and thus, the mechanotransduction of chondrocytes. b) Schematic illustration of cartilage matrix molecular constituents, highlighting the crucial structural role of decorin in regulating both the PCM and T/IT-ECM. The schematics are inspired by Ref. [5, 19, 39].

References

- [1] T. Wang, J.H. Lai, F. Yang, Effects of hydrogel stiffness and extracellular compositions on modulating cartilage regeneration by mixed populations of stem cells and chondrocytes *in vivo*, *Tissue Eng. A* 22 (23-24) (2016) 1348-1356.
- [2] A. Maroudas, Physicochemical properties of articular cartilage, in: M.A.R. Freeman (Ed.), *Adult Articular Cartilage*, Pitman, England, 1979, pp. 215-290.
- [3] D.J. Huey, J.C. Hu, K.A. Athanasiou, Unlike bone, cartilage regeneration remains elusive, *Science* 338 (6109) (2012) 917-921.
- [4] R.E. Wilusz, J. Sanchez-Adams, F. Guilak, The structure and function of the pericellular matrix of articular cartilage, *Matrix Biol.* 39 (2014) 25-32.
- [5] F. Guilak, R.J. Nims, A. Dicks, C.L. Wu, I. Meulenbelt, Osteoarthritis as a disease of the cartilage pericellular matrix, *Matrix Biol.* 71-72 (2018) 40-50.
- [6] Y. Krishnan, A.J. Grodzinsky, Cartilage diseases, *Matrix Biol.* 71-72 (2018) 51-69.
- [7] D.E. Birk, P. Brückner, Collagens, suprastructures, and collagen fibril assembly, in: R.P. Mecham (Ed.), *The Extracellular Matrix: an Overview*, Springer-Verlag, Berlin, 2011, pp. 77-115.
- [8] W. Knudson, S. Ishizuka, K. Terabe, E.B. Askew, C.B. Knudson, The pericellular hyaluronan of articular chondrocytes, *Matrix Biol.* 78-79 (2019) 32-46.
- [9] R.E. Wilusz, S. Zauscher, F. Guilak, Micromechanical mapping of early osteoarthritic changes in the pericellular matrix of human articular cartilage, *Osteoarthritis Cartilage* 21 (12) (2013) 1895-1903.
- [10] D.R. Chery, B. Han, Q. Li, Y. Zhou, S.J. Heo, B. Kwok, P. Chandrasekaran, C. Wang, L. Qin, X.L. Lu, D. Kong, M. Enomoto-Iwamoto, R.L. Mauck, L. Han, Early changes in cartilage pericellular matrix micromechanobiology portend the onset of post-traumatic osteoarthritis, *Acta Biomater.* 111 (2020) 267-278.
- [11] M. Danalache, R. Kleinert, J. Schneider, A.L. Erler, M. Schwitalla, R. Riester, F. Traub, U.K. Hofmann, Changes in stiffness and biochemical composition of the pericellular matrix as a function of spatial chondrocyte organisation in osteoarthritic cartilage, *Osteoarthritis Cartilage* 27 (5) (2019) 823-832.
- [12] M. Urbanczyk, S.L. Layland, K. Schenke-Layland, The role of extracellular matrix in biomechanics and its impact on bioengineering of cells and 3D tissues, *Matrix Biol.* 85-86 (2020) 1-14.
- [13] R.V. Iozzo, M.A. Gubbiotti, Extracellular matrix: the driving force of mammalian diseases, *Matrix Biol.* 71-72 (2018) 1-9.
- [14] N.K. Karamanos, A.D. Theocharis, T. Neill, R.V. Iozzo, Matrix modeling and remodeling: a biological interplay regulating tissue homeostasis and diseases, *Matrix Biol.* 75-76 (2019) 1-11.
- [15] P. Rousselle, M. Montmasson, C. Garnier, Extracellular matrix contribution to skin wound re-epithelialization, *Matrix Biol.* 75-76 (2019) 12-26.
- [16] G. Christensen, K.M. Herum, I.G. Lunde, Sweet, yet underappreciated: proteoglycans and extracellular matrix remodeling in heart disease, *Matrix Biol.* 75-76 (2019) 286-299.
- [17] A. Salustri, L. Campagnolo, F.G. Klinger, A. Camaioni, Molecular organization and mechanical properties of the hyaluronan matrix surrounding the mammalian oocyte, *Matrix Biol.* 78-79 (2019) 11-23.
- [18] S.L. Wunderli, U. Blache, A. Beretta Piccoli, B. Niederöst, C.N. Holenstein, F.S. Passini, U. Silván, L. Bundgaard, U. Auf dem Keller, J.G. Snedeker, Tendon response to matrix unloading is determined by the patho-physiological niche, *Matrix Biol.* 89 (2020) 11-26.
- [19] D. Heinegård, Proteoglycans and more – from molecules to biology, *Int. J. Exp. Pathol.* 90 (6) (2009) 575-586.
- [20] L.G. Alexopoulos, I. Youn, P. Bonaldo, F. Guilak, Developmental and osteoarthritic changes in Col6a1-knockout mice: biomechanics of type VI collagen in the cartilage pericellular matrix, *Arthritis Rheum.* 60 (3) (2009) 771-779.

[21] S.E. Christensen, J.M. Coles, N.A. Zelenski, B.D. Furman, H.A. Leddy, S. Zauscher, P. Bonaldo, F. Guilak, Altered trabecular bone structure and delayed cartilage degeneration in the knees of collagen VI null mice, *PLoS One* 7 (3) (2012) e33397.

[22] N.A. Zelenski, H.A. Leddy, J. Sanchez-Adams, J. Zhang, P. Bonaldo, W. Liedtke, F. Guilak, Type VI collagen regulates pericellular matrix properties, chondrocyte swelling, and mechanotransduction in mouse articular cartilage, *Arthritis Rheumatol.* 67 (5) (2015) 1286-1294.

[23] H. Kaneko, M. Ishijima, I. Futami, N. Tomikawa-Ichikawa, K. Kosaki, R. Sadatsuki, Y. Yamada, H. Kurosawa, K. Kaneko, E. Arikawa-Hirasawa, Synovial perlecan is required for osteophyte formation in knee osteoarthritis, *Matrix Biol.* 32 (3-4) (2013) 178-187.

[24] R. Sadatsuki, H. Kaneko, M. Kinoshita, I. Futami, R. Nonaka, K.L. Culley, M. Otero, S. Hada, M.B. Goldring, Y. Yamada, K. Kaneko, E. Arikawa-Hirasawa, M. Ishijima, Perlecan is required for the chondrogenic differentiation of synovial mesenchymal cells through regulation of Sox9 gene expression, *J. Orthop. Res.* 35 (4) (2017) 837-846.

[25] C.C. Shu, M.T. Jackson, M.M. Smith, S.M. Smith, S. Penn, M.S. Lord, J.M. Whitelock, C.B. Little, J. Melrose, Ablation of perlecan domain 1 heparan sulfate reduces progressive cartilage degradation, synovitis, and osteophyte size in a preclinical model of posttraumatic osteoarthritis, *Arthritis Rheumatol.* 68 (4) (2016) 868-879.

[26] L. Ameye, D. Aria, K. Jepsen, A. Oldberg, T. Xu, M.F. Young, Abnormal collagen fibrils in tendons of biglycan/fibromodulin-deficient mice lead to gait impairment, ectopic ossification, and osteoarthritis, *FASEB J.* 16 (7) (2002) 673-680.

[27] S. Nuka, W. Zhou, S.P. Henry, C.M. Gendron, J.B. Schultz, T. Shinomura, J. Johnson, Y. Wang, D.R. Keene, R. Ramirez-Solis, R.R. Behringer, M.F. Young, M. Hoeoeok, Phenotypic characterization of epiphycan-deficient and epiphycan/biglycan double-deficient mice, *Osteoarthritis Cartilage* 18 (1) (2010) 88-96.

[28] A. Aszódi, J.F. Bateman, E. Hirsch, M. Baranyi, E.B. Hunziker, N. Hauser, Z. Bösze, R. Fässler, Normal skeletal development of mice lacking matrilin 1: redundant function of matrilins in cartilage?, *Mol. Cell. Biol.* 19 (11) (1999) 7841-7845.

[29] Y. Chen, J. Cossman, C.T. Jayasuriya, X. Li, Y. Guan, V. Fonseca, K. Yang, C. Charbonneau, H. Yu, K. Kanbe, P. Ma, E. Darling, Q. Chen, Deficient mechanical activation of anabolic transcripts and post-traumatic cartilage degeneration in matrilin-1 knockout mice, *PLoS One* 11 (6) (2016) e0156676.

[30] Y. Ko, B. Kobbe, C. Nicolae, N. Miosge, M. Paulsson, R. Wagener, A. Aszódi, Matrilin-3 is dispensable for mouse skeletal growth and development, *Mol. Cell. Biol.* 24 (4) (2004) 1691-1699.

[31] P. Li, L. Fleischhauer, C. Nicolae, C. Prein, Z. Farkas, M.M. Saller, W.C. Prall, R. Wagener, J. Heilig, A. Niehoff, H. Clausen-Schaumann, P. Alberton, A. Aszodi, Mice lacking the matrilin family of extracellular matrix proteins develop mild skeletal abnormalities and are susceptible to age-associated osteoarthritis, *Int. J. Mol. Med.* 21 (2) (2008) 666.

[32] N.K. Karamanos, Z. Piperigkou, A.D. Theocharis, H. Watanabe, M. Franchi, S. Baud, S. Brézillon, M. Götte, A. Passi, D. Vigetti, S. Ricard-Blum, R.D. Sanderson, T. Neill, R.V. Iozzo, Proteoglycan chemical diversity drives multifunctional cell regulation and therapeutics, *Chem. Rev.* 118 (18) (2018) 9152-9232.

[33] A.R. Poole, I. Pidoux, A. Reiner, L. Rosenberg, An immunoelectron microscope study of the organization of proteoglycan monomer, link protein, and collagen in the matrix of articular cartilage, *J. Cell Biol.* 93 (3) (1982) 921-937.

[34] T.M. Quinn, A.A. Maung, A.J. Grodzinsky, E.B. Hunziker, J.D. Sandy, Physical and biological regulation of proteoglycan turnover around chondrocytes in cartilage explants. Implications for tissue degradation and repair, *Ann. N. Y. Acad. Sci.* 878 (1) (1999) 420-441.

[35] M.T. Bayliss, S. Howat, C. Davidson, J. Duhdia, The organization of aggrecan in human articular cartilage. Evidence for age-related changes in the rate of aggregation of newly synthesized molecules, *J. Biol. Chem.* 275 (9) (2000) 6321-6327.

[36] L. Ng, A.J. Grodzinsky, P. Patwari, J. Sandy, A. Plaas, C. Ortiz, Individual cartilage aggrecan macromolecules and their constituent glycosaminoglycans visualized via atomic force microscopy, *J. Struct. Biol.* 143 (3) (2003) 242-257.

[37] L. Han, A.J. Grodzinsky, C. Ortiz, Nanomechanics of the cartilage extracellular matrix, *Annu. Rev. Mater. Res.* 41 (2011) 133-168.

[38] T.E. Hardingham, H. Muir, The specific interaction of hyaluronic acid with cartilage proteoglycans, *Biochim. Biophys. Acta* 279 (2) (1972) 401-405.

[39] B. Han, Q. Li, C. Wang, P. Patel, S.M. Adams, B. Doyran, H.T. Nia, R. Oftadeh, S. Zhou, C.Y. Li, X.S. Liu, X.L. Lu, M. Enomoto-Iwamoto, L. Qin, R.L. Mauck, R.V. Iozzo, D.E. Birk, L. Han, Decorin regulates the aggrecan network integrity and biomechanical functions of cartilage extracellular matrix, *ACS Nano* 13 (10) (2019) 11320-11333.

[40] Q. Li, B. Han, C. Wang, W. Tong, W.J. Tseng, L.H. Han, X.S. Liu, M. Enomoto-Iwamoto, R.L. Mauck, L. Qin, R.V. Iozzo, D.E. Birk, L. Han, Mediation of cartilage matrix degeneration and fibrillation by decorin in post-traumatic osteoarthritis, *Arthritis Rheumatol.* 72 (8) (2020) 1266-1277.

[41] D.E. Clapham, Calcium signaling, *Cell* 131 (6) (2007) 1047-1058.

[42] A.J. Hayes, D. Tudor, M.A. Nowell, B. Caterson, C.E. Hughes, Chondroitin sulfate sulfation motifs as putative biomarkers for isolation of articular cartilage progenitor cells, *J. Histochem. Cytochem.* 56 (2) (2008) 125-138.

[43] A.J. Kvist, A. Nyström, K. Hultenby, T. Sasaki, J.F. Talts, A. Aspberg, The major basement membrane components localize to the chondrocyte pericellular matrix — a cartilage basement membrane equivalent?, *Matrix Biol.* 27 (1) (2008) 22-33.

[44] E. Kavanagh, D.E. Ashurst, Development and aging of the articular cartilage of the rabbit knee joint: distribution of biglycan, decorin, and matrilin-1, *J. Histochem. Cytochem.* 47 (12) (1999) 1603-1616.

[45] T. Douglas, S. Heinemann, S. Bierbaum, D. Scharnweber, H. Worch, Fibrillogenesis of collagen types I, II, and III with small leucine-rich proteoglycans decorin and biglycan, *Biomacromolecules* 7 (8) (2006) 2388-2393.

[46] T. Kawamoto, K. Kawamoto, Preparation of thin frozen sections from nonfixed and undecalcified hard tissues using Kawamoto's film method (2012), *Methods Mol. Biol.* 1130 (2014) 149-164.

[47] R.E. Wilusz, L.E. DeFrate, F. Guilak, Immunofluorescence-guided atomic force microscopy to measure the micromechanical properties of the pericellular matrix of porcine articular cartilage, *J. Royal Soc. Interface* 9 (76) (2012) 2997-3007.

[48] C. Wang, B.K. Brisson, M. Terajima, Q. Li, K. Hoxha, B. Han, A.M. Goldberg, X.S. Liu, M.S. Marcolongo, M. Enomoto-Iwamoto, M. Yamauchi, S.W. Volk, L. Han, Type III collagen is a key regulator of the collagen fibrillar structure and biomechanics of articular cartilage and meniscus, *Matrix Biol.* 85-86 (2020) 47-67.

[49] A.K. Williamson, A.C. Chen, R.L. Sah, Compressive properties and function-composition relationships of developing bovine articular cartilage, *J. Orthop. Res.* 19 (6) (2001) 1113-1121.

[50] D. Dean, L. Han, A.J. Grodzinsky, C. Ortiz, Compressive nanomechanics of opposing aggrecan macromolecules, *J. Biomech.* 39 (14) (2006) 2555-2565.

[51] W.A. Hing, A.F. Sherwin, C.A. Poole, The influence of the pericellular microenvironment on the chondrocyte response to osmotic challenge, *Osteoarthritis Cartilage* 10 (4) (2002) 297-307.

[52] S. Otsuki, D.C. Brinson, L. Creighton, M. Kinoshita, R.L. Sah, D. D'Lima, M. Lotz, The effect of glycosaminoglycan loss on chondrocyte viability: a study on porcine cartilage explants, *Arthritis Rheum.* 58 (4) (2008) 1076-1085.

[53] R. Fässler, P.N.J. Schnegelsberg, J. Dausman, T. Shinya, Y. Muragaki, M.T. McCarthy, B.R. Olsen, R. Jaenisch, Mice lacking $\alpha 1$ (IX) collagen develop noninflammatory degenerative joint disease, *Proc. Natl. Acad. Sci. USA* 91 (11) (1994) 5070-5074.

[54] L. Xu, C.M. Flahiff, B.A. Waldman, D. Wu, B.R. Olsen, L.A. Setton, Y. Li, Osteoarthritis-like changes and decreased mechanical function of articular cartilage in the joints of mice with the chondrodysplasia gene (*cho*), *Arthritis Rheum.* 48 (9) (2003) 2509-2518.

[55] C. Wiberg, E. Hedbom, A. Khairullina, S.R. Lamande, A. Oldberg, R. Timpl, M. Mörgelin, D. Heinegård, Biglycan and decorin bind close to the N-terminal region of the collagen VI triple helix, *J. Biol. Chem.* 276 (22) (2001) 18947-18952.

[56] C. Wiberg, A.R. Klatt, R. Wagener, M. Paulsson, J.F. Bateman, D. Heinegård, M. Mörgelin, Complexes of matrilin-1 and biglycan or decorin connect collagen VI microfibrils to both collagen II and aggrecan, *J. Biol. Chem.* 278 (39) (2003) 37698-37704.

[57] C.J. O'Conor, H.A. Leddy, H.C. Benefield, W.B. Liedtke, F. Guilak, TRPV4-mediated mechanotransduction regulates the metabolic response of chondrocytes to dynamic loading, *Proc. Natl. Acad. Sci. USA* 111 (4) (2014) 1316-1321.

[58] W. Lee, H.A. Leddy, Y. Chen, S.H. Lee, N.A. Zelenski, A.L. McNulty, J. Wu, K.N. Beicker, J. Coles, S. Zauscher, J. Grandl, F. Sachs, F. Guilak, Synergy between Piezo1 and Piezo2 channels confers high-strain mechanosensitivity to articular cartilage, *Proc. Natl. Acad. Sci. USA* 111 (47) (2014) E5114-E5122.

[59] C.J. O'Conor, S. Ramalingam, N.A. Zelenski, H.C. Benefield, I. Rigo, D. Little, C.L. Wu, D. Chen, W. Liedtke, A.L. McNulty, F. Guilak, Cartilage-specific knockout of the mechanosensory ion channel TRPV4 decreases age-related osteoarthritis, *Sci. Rep.* 6 (2016) 29053.

[60] F. Guilak, L.G. Alexopoulos, M.L. Upton, I. Youn, J.B. Choi, L. Cao, L.A. Setton, M.A. Haider, The pericellular matrix as a transducer of biomechanical and biochemical signals in articular cartilage, *Ann. N. Y. Acad. Sci.* 1068 (2006) 498-512.

[61] Y. Zhou, M. Lv, T. Li, T. Zhang, R. Duncan, L. Wang, X.L. Lu, Spontaneous calcium signaling of cartilage cells: from spatiotemporal features to biophysical modeling, *FASEB J.* 33 (4) (2019) 4675-4687.

[62] J.F. Weber, S.D. Waldman, Calcium signaling as a novel method to optimize the biosynthetic response of chondrocytes to dynamic mechanical loading, *Biomech. Model. Mechanobiol.* 13 (6) (2014) 1387-1397.

[63] R.F. Loeser, S. Sadiev, L. Tan, M.B. Goldring, Integrin expression by primary and immortalized human chondrocytes: evidence of a differential role for $\alpha 1\beta 1$ and $\alpha 2\beta 1$ integrins in mediating chondrocyte adhesion to types II and VI collagen, *Osteoarthritis Cartilage* 8 (2) (2000) 96-105.

[64] M.A. Gubbiotti, T. Neill, R.V. Iozzo, A current view of perlecan in physiology and pathology: a mosaic of functions, *Matrix Biol.* 57-58 (2017) 285-298.

[65] T.L. Vincent, C.J. McLean, L.E. Full, D. Peston, J. Saklatvala, FGF-2 is bound to perlecan in the pericellular matrix of articular cartilage, where it acts as a chondrocyte mechanotransducer, *Osteoarthritis Cartilage* 15 (7) (2007) 752-763.

[66] X. Xu, Z. Li, Y. Leng, C.P. Neu, S. Calve, Knockdown of the pericellular matrix molecule perlecan lowers *in situ* cell and matrix stiffness in developing cartilage, *Dev. Biol.* 418 (2) (2016) 242-247.

[67] R.V. Iozzo, S. Goldoni, A.D. Berendsen, M.F. Young, Small leucine-rich proteoglycans, in: R.F. Mecham (Ed.), *The Extracellular Matrix: an Overview*, Springer-Verlag, Berlin, 2011, pp. 197-231.

[68] G. Zhang, Y. Ezura, I. Chervoneva, P.S. Robinson, D.P. Beason, E.T. Carine, L.J. Soslowsky, R.V. Iozzo, D.E. Birk, Decorin regulates assembly of collagen fibrils and acquisition of biomechanical properties during tendon development, *J. Cell. Biochem.* 98 (6) (2006) 1436-1449.

[69] K.A. Robinson, M. Sun, C.E. Barnum, S.N. Weiss, J. Huegel, S.S. Shetye, L. Lin, D. Saez, S.M. Adams, R.V. Iozzo, L.J. Soslowsky, D.E. Birk, Decorin and biglycan are necessary for

maintaining collagen fibril structure, fiber realignment, and mechanical properties of mature tendons, *Matrix Biol.* 64 (2017) 81-93.

[70] G. Zhang, S. Chen, S. Goldoni, B.W. Calder, H.C. Simpson, R.T. Owens, D.J. McQuillan, M.F. Young, R.V. Iozzo, D.E. Birk, Genetic evidence for the coordinated regulation of collagen fibrillogenesis in the cornea by decorin and biglycan, *J. Biol. Chem.* 284 (13) (2009) 8879-8888.

[71] G. Barreto, A. Soininen, P. Ylinen, J. Sandelin, Y.T. Konttinen, D.C. Nordstrom, K.K. Eklund, Soluble biglycan: a potential mediator of cartilage degradation in osteoarthritis, *Arthritis Res. Ther.* 17 (1) (2015) 379.

[72] T. Gronau, K. Kruger, C. Prein, A. Aszodi, I. Gronau, R.V. Iozzo, F.C. Mooren, H. Clausen-Schaumann, J. Bertrand, T. Pap, P. Bruckner, R. Dreier, Forced exercise-induced osteoarthritis is attenuated in mice lacking the small leucine-rich proteoglycan decorin, *Ann. Rheum. Dis.* 76 (2) (2017) 442-449.

[73] M. Loparic, D. Wirz, A.U. Daniels, R. Raiteri, M.R. VanLandingham, G. Guex, I. Martin, U. Aebi, M. Stolz, Micro- and nanomechanical analysis of articular cartilage by indentation-type atomic force microscopy: validation with a gel-microfiber composite, *Biophys. J.* 98 (11) (2010) 2731-2740.

[74] M. Stolz, R. Gottardi, R. Raiteri, S. Miot, I. Martin, R. Imer, U. Staufer, A. Raducanu, M. Düggelin, W. Baschong, A.U. Daniels, N.F. Friederich, A. Aszodi, U. Aebi, Early detection of aging cartilage and osteoarthritis in mice and patient samples using atomic force microscopy, *Nat. Nanotechnol.* 4 (3) (2009) 186-192.

[75] H.T. Nia, S.J. Gauci, M. Azadi, H.-H. Hung, E. Frank, A.J. Fosang, C. Ortiz, A.J. Grodzinsky, High-bandwidth AFM-based rheology is a sensitive indicator of early cartilage aggrecan degradation relevant to mouse models of osteoarthritis, *J. Biomech.* 48 (2015) 162-165.

[76] M.A. Batista, H.T. Nia, P. Önnerfjord, K.A. Cox, C. Ortiz, A.J. Grodzinsky, D. Heinegård, L. Han, Nanomechanical phenotype of chondroadherin-null murine articular cartilage, *Matrix Biol.* 38 (2014) 84-90.

[77] B. Doyran, W. Tong, Q. Li, H. Jia, X. Zhang, C. Chen, M. Enomoto-Iwamoto, X.L. Lu, L. Qin, L. Han, Nanoindentation modulus of murine cartilage: a sensitive indicator of the initiation and progression of post-traumatic osteoarthritis, *Osteoarthritis Cartilage* 25 (1) (2017) 108-117.

[78] L. Cao, I. Youn, F. Guilak, L.A. Setton, Compressive properties of mouse articular cartilage determined in a novel micro-indentation test method and biphasic finite element model, *J. Biomech. Eng.* 128 (5) (2006) 766-771.

[79] K. Hu, L. Xu, L. Cao, C.M. Flahiff, J. Brussiau, K. Ho, L.A. Setton, I. Youn, F. Guilak, B.R. Olsen, Y. Li, Pathogenesis of osteoarthritis-like changes in the joints of mice deficient in type IX collagen, *Arthritis Rheum.* 54 (9) (2006) 2891-2900.

[80] R.L. Mauck, S.B. Nicoll, S.L. Seyhan, G.A. Ateshian, C.T. Hung, Synergistic action of growth factors and dynamic loading for articular cartilage tissue engineering, *Tissue Eng.* 9 (4) (2003) 597-611.

[81] D.E. Anderson, B. Johnstone, Dynamic mechanical compression of chondrocytes for tissue engineering: a critical review, *Front. Bioeng. Biotechnol.* 5 (2017) 76.

[82] Z. Zhang, Chondrons and the pericellular matrix of chondrocytes, *Tissue Eng. B Rev.* 21 (3) (2015) 267-277.

[83] A.H. Huang, M.J. Farrell, M. Kim, R.L. Mauck, Long-term dynamic loading improves the mechanical properties of chondrogenic mesenchymal stem cell-laden hydrogel, *Eur. Cell Mater.* 19 (2010) 72-85.

[84] O.M. Babalola, L.J. Bonassar, Effects of seeding density on proteoglycan assembly of passaged mesenchymal stem cells, *Cell. Mol. Bioeng.* 3 (3) (2010) 197-206.

[85] C.N. Salinas, K.S. Anseth, Decorin moieties tethered into PEG networks induce chondrogenesis of human mesenchymal stem cells, *J. Biomed. Mater. Res. A* 90 (2) (2009) 456-464.

[86] L.A. Fortier, J.U. Barker, E.J. Strauss, T.M. McCarrel, B.J. Cole, The role of growth factors in cartilage repair, *Clin. Orthop. Relat. Res.* 469 (10) (2011) 2706-2715.

[87] A. Hildebrand, M. Romarís, L.M. Rasmussen, D. Heinegård, D.R. Twardzik, W.A. Border, E. Ruoslahti, Interaction of the small interstitial proteoglycans biglycan, decorin and fibromodulin with transforming growth factor β , *Biochem. J.* 302 (1994) 527-534.

[88] S.L. Vega, M.Y. Kwon, J.A. Burdick, Recent advances in hydrogels for cartilage tissue engineering, *Eur. Cell Mater.* 33 (2017) 59-75.

[89] J.C. Ashworth, J.L. Thompson, J.R. James, C.E. Slater, S. Pijuan-Galitó, K. Lis-Slimak, R.J. Holley, K.A. Meade, A. Thompson, K.P. Arkill, M. Tassieri, A.J. Wright, G. Farnie, C.L.R. Merry, Peptide gels of fully-defined composition and mechanics for probing cell-cell and cell-matrix interactions in vitro, *Matrix Biol.* 85-86 (2020) 15-33.

[90] A.J. Berger, C.M. Renner, I. Hale, X. Yang, S.M. Ponik, P.S. Weisman, K.S. Masters, P.K. Kreeger, Scaffold stiffness influences breast cancer cell invasion via EGFR-linked Mena upregulation and matrix remodeling, *Matrix Biol.* 85-86 (2020) 80-93.

[91] R.L. Mauck, M.A. Soltz, C.C.B. Wang, D.D. Wong, P.H.G. Chao, W.B. Valhmu, C.T. Hung, G.A. Ateshian, Functional tissue engineering of articular cartilage through dynamic loading of chondrocyte-seeded agarose gels, *J. Biomech. Eng.* 122 (3) (2000) 252-260.

[92] M.A. Gubbiotti, S.D. Vallet, S. Ricard-Blum, R.V. Iozzo, Decorin interacting network: a comprehensive analysis of decorin-binding partners and their versatile functions, *Matrix Biol.* 55 (2016) 7-21.

[93] K. Pietraszek-Gremplewicz, K. Karamanou, A. Niang, M. Dauchez, N. Belloy, F.X. Maquart, S. Baud, S. Brézillon, Small leucine-rich proteoglycans and matrix metalloproteinase-14: key partners?, *Matrix Biol.* 75-76 (2019) 271-285.

[94] S. Buraschi, T. Neill, R.V. Iozzo, Decorin is a devouring proteoglycan: remodeling of intracellular catabolism via autophagy and mitophagy, *Matrix Biol.* 75-76 (2019) 260-270.

[95] F. Cianfarani, E. De Domenico, A. Nyström, S. Mastroeni, D. Abeni, E. Baldini, S. Ulisse, P. Uva, L. Bruckner-Tuderman, G. Zambruno, D. Castiglia, T. Odorisio, Decorin counteracts disease progression in mice with recessive dystrophic epidermolysis bullosa, *Matrix Biol.* 81 (2019) 3-16.

[96] S. Patel, M. Santra, D.J. McQuillan, R.V. Iozzo, A.P. Thomas, Decorin activates the epidermal growth factor receptor and elevates cytosolic Ca^{2+} in A431 carcinoma cells, *J. Biol. Chem.* 273 (6) (1998) 3121-3124.

[97] G. Csordás, M. Santra, C.C. Reed, I. Eichstetter, D.J. McQuillan, D. Gross, M.A. Nugent, G. Hajnóczky, R.V. Iozzo, Sustained down-regulation of the epidermal growth factor receptor by decorin. A mechanism for controlling tumor growth in vivo, *J. Biol. Chem.* 275 (42) (2000) 32879-32887.

[98] K.G. Danielson, H. Baribault, D.F. Holmes, H. Graham, K.E. Kadler, R.V. Iozzo, Targeted disruption of decorin leads to abnormal collagen fibril morphology and skin fragility, *J. Cell Biol.* 136 (3) (1997) 729-743.

[99] E.J. Vanderploeg, C.G. Wilson, S.M. Imler, C.H. Ling, M.E. Levenston, Regional variations in the distribution and colocalization of extracellular matrix proteins in the juvenile bovine meniscus, *J. Anat.* 221 (2) (2012) 174-186.

[100] H.L. Ansorge, X. Meng, G. Zhang, G. Veit, M. Sun, J.F. Klement, D.P. Beason, L.J. Soslowsky, M. Koch, D.E. Birk, Type XIV collagen regulates fibrillogenesis: premature collagen fibril growth and tissue dysfunction in null mice, *J. Biol. Chem.* 284 (13) (2009) 8427-8438.

[101] E.K. Dimitriadis, F. Horkay, J. Maresca, B. Kachar, R.S. Chadwick, Determination of elastic moduli of thin layers of soft material using the atomic force microscope, *Biophys. J.* 82 (5) (2002) 2798-2810.

[102] W.M. Han, S.J. Heo, T.P. Driscoll, J.F. Delucca, C.M. McLeod, L.J. Smith, R.L. Duncan, R.L. Mauck, D.M. Elliott, Microstructural heterogeneity directs micromechanics and mechanobiology in native and engineered fibrocartilage, *Nat. Mater.* 15 (4) (2016) 477-484.

[103] R.W. Farndale, D.J. Buttle, A.J. Barrett, Improved quantitation and discrimination of sulfated glycosaminoglycans by use of dimethylmethylene blue, *Biochim. Biophys. Acta* 883 (2) (1986) 173-177.

[104] D. Bates, M. Mächler, B.M. Bolker, S.C. Walker, Fitting linear mixed-effects models using lme4, *J. Stat. Softw.* 67 (1) (2015) 1-48.

Journal Pre-proof